Tolerance Optimization of Supersonic ORC Turbine Stator

Nassim Razaaly[1(✉)], Giacomo Persico[2], and Pietro Marco Congedo[1]

[1] Inria Saclay IDF, Palaiseau, France
{nassim.razaaly,pietro.congedo}@inria.fr
[2] Politecnico di Milano, Milan, Italy
giacomo.persico@polimi.it

Abstract. The discrepancy between manufactured and design geometry of turbomachinery blades has a detrimental effect on the performance variability. In this work, the authors propose a methodology to reduce the impact of the randomness induced by the manufacturing process: a *tolerance* optimization is carried out by resorting to an efficient robust optimization method based on quantile regression. Its application to a typical two-dimensional supersonic nozzle cascade for ORC showcases promising preliminary results.

Keywords: ORC Stator · Quantile regression · NICFD · Robust optimization · Random field · Geometric uncertainty

1 Introduction

The geometry of manufactured turbomachinery blades inevitably differs from the design geometry, due to noise in the manufacturing process or in-service erosion. It generally induces both an increase in performance variability while decreasing its mean performance. Garzon [5] demonstrated that the mean loss coefficient of a flank-milled integrally bladed rotor (IBR) increased by 23% due to manufacturing variability. Dow proposed a robust design framework combining both geometric and tolerance optimization of a compressor exit vane, leading to a quite large number of flow simulations performed using the Multiple Blade Interacting Streamtube Euler Solver (MISES) code [3]. Similarly to Dow, we assume that the geometric variability in manufactured turbine blades can be described as a non-stationary Gaussian Random Field, representing the error between the manufactured surface and the nominal (perfect) one, fully defined by its autocovariance function.

The effect of tightening manufacturing tolerances is modelled by reducing the standard deviation of the random field locally. This work focuses on the tolerance optimization by resorting to a Robust Optimization (RO) based on Quantile Regression [14], yielding a low number of CFD simulations. The proposed method permits to quantitatively highlight the regions of the blade that have the largest impact on the average performance.

This methodology is applied to a typical supersonic nozzle cascade for ORC applications, using the popular NICFD flow solver SU2. Indeed, the peculiarities of organic

M. Pini et al. (Eds.): NICFD 2020, ERCOFTAC Series 28, pp. 78–86, 2021.
https://doi.org/10.1007/978-3-030-69306-0_9

fluids typically lead to supersonic turbine configurations featuring supersonic flows and shocks, which can be influenced by the geometric tolerances of the blade manufacturing, as emphasized in [11].

The supersonic nature of the blade makes the throat zone, especially in the supersonic area downstream the throat (both in the divergent and in the semi-bladed part), very *sensitive* to the geometry. This behavior might be exploited in the manufacturing phase, only if the effect is appropriately modeled and quantified. This long term objective motivates the present research work.

In this paper, we propose an efficient framework for the robust design of the tolerances of a two-dimensional nozzle cascade. The originality w.r.t. [3] lies in the use of a parcimonious RO method combined with an original parametrization of the design space.

2 Methodology

The NICFD test-case is described in Subsect. 2.1. The uncertainty framework and in particular the description of the perturbed blades generation from a given design vector is fully presented in Subsect. 2.2. The robust optimization method is described in Subsect. 2.3.

2.1 NICFD Case Description

The targeted Organic Rankine Cycle (ORC) turbine is the geometry of an existing ORC stator designed for a 300 kWe Combined-Heat-and-Power axial turbogenerator employing siloxane MDM as working fluid (whose properties are reported in Table 1). This supersonic axial-flow turbine stator is characterized by converging-diverging blades and it features significant fluid-dynamic penalties due to a strong shock-wave forming on the rear suction side of the blade. This exemplary profile, originally presented in [1] has been extensively studied in the open literature of ORC. In recent years, it has been subjected to several deterministic optimization trials [9,16] and robust ones in [10,12]. The flow model focuses on the two-dimensional flow around the blade profiles at the midspan section of the cascade considering operating conditions provided in Table 1.

In order to estimate the aerodynamic performances of the supersonic turbine, the Non-Ideal Compressible-Fluid Dynamics solver included in the SU2 [4,8,17] suite is employed, embedding in particular the Peng-Robinson-Stryjek-Vera Equation of State to describe the fluid thermodynamic behavior. Inviscid fluxes are discretized using a MUSCL approach based on an approximate Riemann solver of Roe upwind type [7,13,15] along with the slope limiter proposed by van Albada. Additionally, Non-Reflecting Boundary Conditions [6] are exploited to avoid spurious pressure oscillations due to the reflection of spurious pressure waves at domain boundaries. The unstructured grids are generated using an in-house tool based on an advancing-front/Delaunay algorithm. Inviscid simulations are performed using a restart file corresponding to the baseline simulation, on meshes constituted of 16k cells, selected in [12] after grid dependence study, as optimal trade-off between accuracy and cost (Table 2).

Table 1. MDM gas properties and operating conditions.

Critical pressure	14.152 bar
Critical temperature	564.1 K
Critical density	256.82 kg.m^{-3}
γ	1.0165
Acentric factor ω	0.529
Gas constant	35.152 J/kg/K
μ	1.1517×10^{-5} Pa.s
k	0.03799 W/(m.K)
Inlet total pressure [Pa]	8×10^5
Inlet total temperature [K]	545.15
Inlet axial angle [°]	0
Outlet static pressure [Pa]	1.072×10^5

Table 2. Test-case: mach contours and 16k cells mesh.

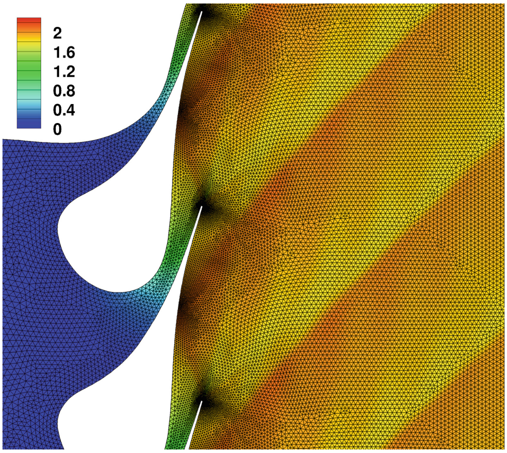

The Quantity of Interest (QoI) considered is the standard deviation of the distribution of the static pressure measured half-axial chord downstream the blade, denoted as ΔP. This objective function is selected since minimizing it directly increases the performance of the stator as it minimizes the impact of the shock, which is the main source of loss here. It also has a beneficial effect on the downstream rotor, as it makes the flow entering it more uniform. Figure 2 illustrates the NICFD test-case by providing the Mach contours and showcasing the mesh.

2.2 Modeling Geometric Variability

2.2.1 Random Field Generation

Following [2,3,11], we assume that the geometric variability in manufactured turbine blades can be accurately described as a *non-stationary Gaussian Random Field* $e(s,\omega)$, ω being a coordinate in the sample space Ω, and $(\Omega, \mathscr{F}, \mathbb{P})$ a complete probability space. The arclength $s \in [0,1]$ parametrizes the location on the blade surface, starting at the trailing edge ($s = 0$), going around the leading edge ($s = \frac{1}{2}$), and continuing back to the trailing edge on the opposite side of the blade ($s = 1$).

The Random field $e(s,\omega)$ represents the error between the manufactured surface and the nominal (perfect) one in the normal direction at the point parametrized by s. It is fully defined by its mean $\bar{e}(s)$ (null here) and autocovariance function $C(s,t)$: it captures the correlation between manufacturing errors at locations along the blade surface parametrized by $s, t \in [0,1]$, and describes the smoothness and correlation length of the random field. It is written as [11]:

$$C(s,t) = \sigma(s)\ \sigma(t)\ \rho(s,t) \quad (1)$$

where $\sigma(s)$ is the standard deviation of the random field at location s, which quantifies locally the level of manufacturing variability. Its modeling is described in Subsect. 2.2.2, and is the goal of the present work. The non-stationary autocorrelation function ρ is defined by:

$$\rho(s,t) = \exp\left(-\frac{|s-t|^2}{L(s)L(t)}\right) \tag{2}$$

where

$$L(s) = L_0 + (L_{LE} - L_0)\exp\left(-\frac{|s-\frac{1}{2}|^2}{w^2}\right) \tag{3}$$

The values $L_0 = 0.1$, $w = 0.1$ and $L_{LE} = 1.0 \times 10^{-2}$, all normalized by the blade half-arclength were used [11]. In the present study, the trailing edge is modeled as a straight segment, thus, the impact of manufacturing variability at the trailing edge is not addressed.

In order to sample a random field $e(\bullet,\omega)$ on a set $\mathscr{S} = \{s_1,...,s_{n_{blade}}\}$, representing the values in $[0,1]$ parametrizing the n_{blade} nodes on the blade profile, the following procedure is applied:

- The discrete covariance matrix $\mathbf{C} = [C(s_i,s_j)]_{i\in[\![1,n_{blade}]\!]}$ is generated.
- A gaussian vector $g \in \mathbb{R}^{n_{blade}}$ is generated, with $g \sim \mathscr{N}(0,\mathbf{C})$.

For more details, the reader is referred to [11].

2.2.2 $\sigma(s)$ Parametrization: Design Vector

A standard approach [11] consists in assuming a constant standard deviation of the random field: $\sigma(s) = \sigma_0$, for a given constant $\sigma_0 = 3\times 10^{-5}m$ here. The goal of the present work is to find an optimal distribution of $\sigma(\bullet)$ leading to a reduced detrimental impact of geometric variability on the prescribed blade profile, satisfying a (manufacturing) cost constraint. Here we simply search for a distribution satisfying $\int_{[0,1]}\sigma(s)ds = \sigma_0$. A two-degree of freedom parametrization is chosen here, based:

$$\sigma_{\mathbf{x}}(s) = \sigma_0 + b(s,\mathbf{x}) \tag{4}$$

where $b(s,\mathbf{x})$ is a cubic Béziers curve in $[0,1]$, defined by 4 so-called control points $P_0,P_1,P_2,P_3 \in \mathbb{R}^2$:

$$b(s,\mathbf{x}) = P_0(1-s)^3 + 3P_1 s(1-s)^2 + 3P_2 s^2(1-s) + P_3 s^3. \tag{5}$$

To ensure $\int_{[0,1]}\underline{\ }(s,\mathbf{x})ds = 0$, we choose $P_0 = (0,x_2)$, $P_1 = (0.5-x_0,x_1)$, $P_2 = (0.5+x_0,-x_1)$ and $P_3 = (0,-x_2)$, with $\mathbf{x} = (x_0,x_1,x_2)$ denoting the design vector. The design space is chosen as $\Omega = [-3,3]\times[-2\sigma_0,2\sigma_0]\times[\sigma_0,\sigma_0]$. Figure 1 provides an illustration of this parametrization, and the corresponding influence of the local level of manufacturing variability on the blade. In the following, a random field as described in Subsect. 2.2.1 based on the standard deviation $\sigma_{\mathbf{x}}(s)$ is denoted by $e_{\mathbf{x}}(s,\omega)$.

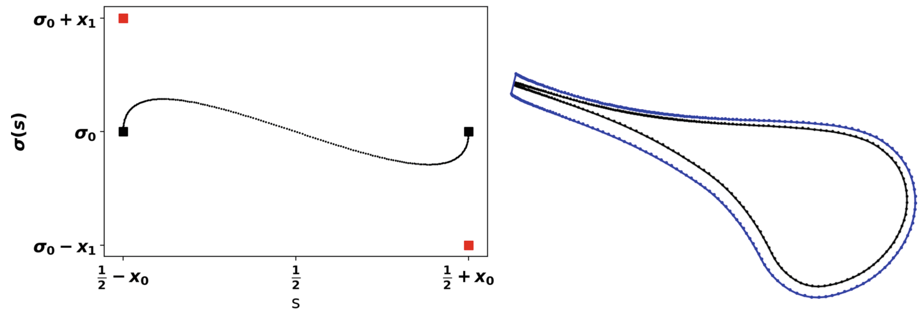

(a) 1D Representation (b) Blade

Fig. 1. Random Field Illustration. (a) Distribution $\sigma_{\mathbf{x}}(s)$, with $\mathbf{x} = (0.5, 2\sigma_0, 0)$. (b) Blade geometry. Baseline (black) and corresponding $\sigma_{\mathbf{x}}(s)$ perturbation (blue) with scale = 50.

Figure 2 presents examples of realizations for a given design vector.

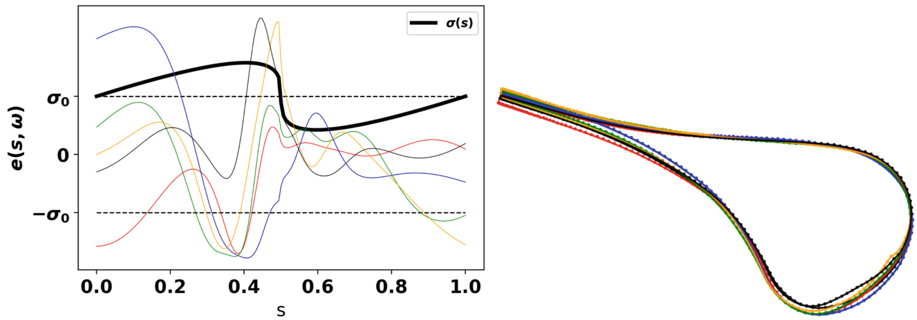

(a) 1D Representation (b) Blade

Fig. 2. Random field realizations: $\mathbf{x} = (0.5, 2\sigma_0, 0)$, scale = 20.

2.2.3 Stochastic Model

For a given design vector $\mathbf{x}$, a random field $e_{\mathbf{x}}$ is defined based on its local standard deviation distribution $\sigma_{\mathbf{x}}(\bullet)$. A geometric error realization $e_{\mathbf{x}}(\bullet, \omega^*(\mathbf{x})$ following $e_{\mathbf{x}}$ is then sampled, corresponding to a perturbed blade geometry, where $\omega^*(\mathbf{x})$ representing a coordinate in the sample space depending on $\mathbf{x}$. A CFD simulation permits the evaluation of the QoI $\Delta P(\mathbf{x}, \omega^*(\mathbf{x})$, or simply the random QoI $\Delta P(\mathbf{x})$. In other terms, $\mathbf{x} \mapsto \Delta P(\mathbf{x})$ can be represented as a scalar stochastic model, as several simulations of the same input normally result in different outputs.

2.3 (Robust) Optimization Framework

The objective of the present work is to find an optimal distribution of the standard deviation of the random field describing the geometric discrepancy between manufactured blades and the nominal (perfect) one. Such optimal distribution would permit to limit the detrimental effect on the variability of the scalar random QoI ΔP. We propose to recast this problem as a robust optimization one, formulated as follows:

$$\begin{aligned} \text{Minimize} \;\; & q_{80}[\Delta P(\mathbf{x})] \\ \text{s.t.} \;\; & \mathbf{x} \in \Omega \subset \mathbb{R}^3 \end{aligned} \tag{6}$$

where q_{80} is the 80% quantile operator induced by the random field $e_{\mathbf{x}}$. Other statistics could have been chosen, such as linear combination of the mean and standard deviation, other quantiles... In order to solve Eq. 6, we resort to a methodology based on Quantile Regression (QR) [14] for Robust Optimization. This method is suitable for low dimensional design space, and high dimensional (possibly non-parametric) stochastic space, which is consistent with the problem we propose to solve. An initial Design of Experiment (DoE) of size $n0 = 300$ is first generated $\mathscr{T} = \{\mathbf{x}_i, \Delta P(\mathbf{x}_i)\}_i$, based on Latin Hypercube Sampling (LHS). A QR based on $n_{CP} = 37$ so-called Control Points is built. The seminal work described in [14] is slightly modified: the bayesian description of the QR enabling to obtain uncertainties in the QR derivation based on so-called Markov-Chain Monte-Carlo (MCMC) is replaced by building several QR representations based on random generation of the Control Points. It enables to cheaply obtain an estimation of the mean and quantiles of the QR, used to select promising designs. At each optimization iteration, $K = 8$ CFD runs are performed to update the DoE.

3 Results

Some preliminary results are presented: the optimal configuration is compared w.r.t. the baseline one $\mathbf{x}_0$, which corresponds to a constant standard deviation distribution, *i. e.* $\sigma(s) = \sigma_0$. The robust optimization framework required 38 iterations to converge, for which 8 CFD simulations are run in parallel in less than 2 m, so that the final number of CFD run is $nf = 604$. To assess the quantile results for both the baseline $\mathbf{x}_0$ and the optimal design $\mathbf{x}^*$, 200 samples following respectively $e_{\mathbf{x}_0}$ and $e_{\mathbf{x}^*}$ are generated and assessed by the NICFD solver. First, the so-called Probability Density Function (PDF) of the QoI ΔP is built, as the empiric 80% quantile, as reproduced in Fig. 3(a). We can observe that the PDF corresponding to the optimized design is significantly less spread than for the baseline configuration, while the difference between both quantiles is small (0.15%). This noticeable favorable impact may be due to the choice of a high quantile for the statistics. Same comments apply to the total loss pressure coefficient Y PDF 3(b).

Figure 5 represents the local distribution of the standard deviation for the optimized case, and examples of realizations of perturbed blade geometries.

To exhibit the impact of the distribution of the standard deviation on the blade aerodynamics, the contours of Coefficient of Variation (CoV) of the Mach number is presented in Fig. 4, with $Cov = \dfrac{\sigma}{\mu}$. The CoV values are estimated locally at the nodes of the mesh, using standard empirical estimators. The Mach CoV for the baseline in Fig. 4(a) is very similar to the analysis obtained in [11] from a RANS simulation. The result obtained for the optimized design emphasizes that the CoV increases in the shock zone, while it decreases in the isentropic region upstream the blade and at the beginning of the bladed channel.

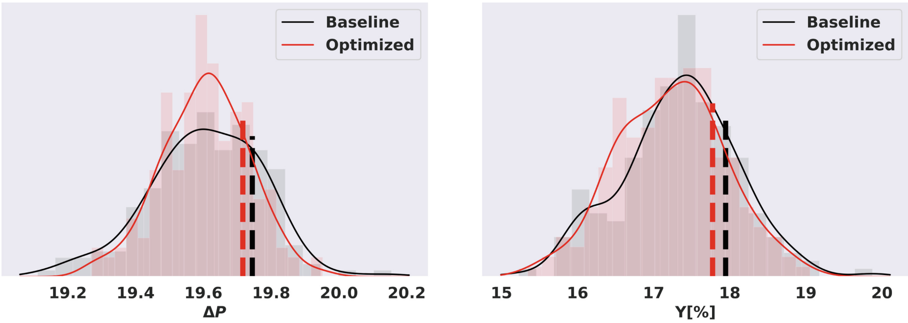

(a) ΔP PDF (b) Y PDF

Fig. 3. PDF of the QOIs ΔP (a) and total pressure loss Y (d): baseline design $\mathbf{x}_0$ (black) and optimal design $\mathbf{x}^*$ (red). The vertical line exhibits the 80% quantile.

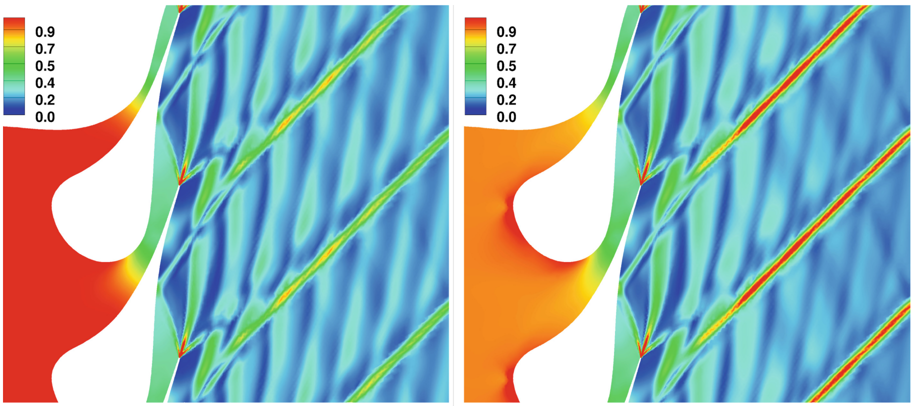

(a) Baseline (b) Optimized

Fig. 4. Contours of mach CoV[%] for the baseline and the optimal designs, based on 200 CFD samples.

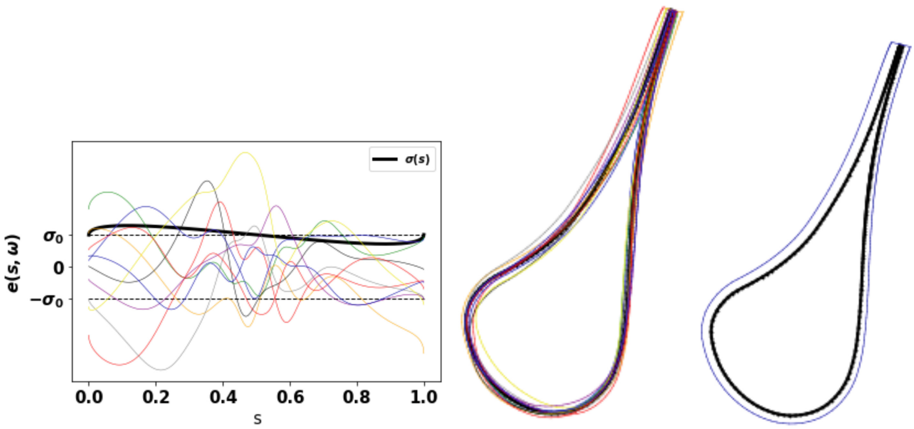

(a) 1D Representation (b) Blade (c) Standard Deviation

Fig. 5. Optimized design: random field realizations and local distribution of the standard deviation (scale = 20).

4 Conclusions and Future Works

The present research work proposed a methodology for optimizing the distribution of the *geometric variability*. This problem is solved by resorting to a modified state-of-the-art robust optimization method based on QR. We demonstrated its impact applying it to a two-dimensional nozzle cascade, using an inviscid NICFD solver. The robust optimization problem, characterized by a design space of small dimensionality ($d = 3$) and large stochastic dimension, required at total of 608 CFD evaluations: $n_0 = 300$ for the initialization, and 37 iterations of $K = 8$ CFD runs performed in parallel. A significant improvement of the statistics and the PDF of the QOIs is obtained. Those are still preliminary results. Future work will consist mainly in improving the parametrization of the design space and considering RANS simulations.

References

1. Colonna, P., Harinck, J., Rebay, S., Guardone, A.: Real-gas effects in organic Rankine cycle turbine nozzles. J. Propul. Power **24**(2), 282–294 (2008)
2. Dow, E.A., Wang, Q.: Optimal design and tolerancing of compressor blades subject to manufacturing variability. In: 16th AIAA Non-Deterministic Approaches Conference, p. 1008 (2014)
3. Dow, E.A., Wang, Q.: The implications of tolerance optimization on compressor blade design. J. Turbomach. **137**(10) (2015)
4. Economon, T.D., Mudigere, D., Bansal, G., Heinecke, A., Palacios, F., Park, J., Smelyanskiy, M., Alonso, J.J., Dubey, P.: Performance optimizations for scalable implicit RANS calculations with SU2. Comput. Fluids **129**, 146–158 (2016)
5. Garzon, V.E.: Probabilistic aerothermal design of compressor airfoils. PhD thesis, Massachusetts Institute of Technology (2003)

6. Giles, M.B.: Nonreflecting boundary conditions for Euler equation calculations. AIAA J. **28**(12), 2050–2058 (1990)
7. Guardone, A., Vigevano, L.: Roe linearization for the van der Waals gas. J. Comput. Phys. **175**, 50–78 (2002)
8. Palacios, F., Colonno, M.F., Aranake, A.C., Campos, A., Copeland, S.R., Economon, T.D., Lonkar, A.K., Lukaczyk, T.W., Taylor, T.W.R., Alonso, J.J.: Stanford university unstructured (SU2): an open-source integrated computational environment for multi-physics simulation and design. In: 51st AIAA Aerospace Sciences Meeting and Exhibit (2013)
9. Persico, G., Rodriguez-Fernandez, P., Romei, A.: High-fidelity shape optimization of non-conventional turbomachinery by surrogate evolutionary strategies. J. Turbomach. **141**(8), 081010–0810111 (2019)
10. Pini, M., Persico, G., Dossena, V.: Robust adjoint-based shape optimization of supersonic turbomachinery cascades. In: ASME Turbo Expo 2014: Turbine Technical Conference and Exposition, pp. V02BT39A043–V02BT39A043. American Society of Mechanical Engineers (2014)
11. Razaaly, N., Persico, G., Congedo, P.M.: Impact of geometric, operational, and model uncertainties on the non-ideal flow through a supersonic ORC turbine cascade. Energy **169**, 213–227 (2019)
12. Razaaly, N., Persico, G., Gori, G., Congedo, P.M.: Quantile-based robust optimization of a supersonic nozzle for organic Rankine cycle turbines. Appl. Math. Model **82**, 802–824 (2020)
13. Roe, P.L.: Approximate Riemann solvers, parameter vectors, and difference schemes. J. Comput. Phys. **43**(2), 357–372 (1981)
14. Sabater, C., Le Maitre, O., Congedo, P.M., Gortz, S.: A Bayesian approach for quantile optimization problems with high-dimensional uncertainty sources. Researchgate (2020)
15. Vinokur, M., Montagné, J.L.: Generalized flux-vector splitting and roe average for an equilibrium real gas. J. Comput. Phys. **89**, 276 (1990)
16. Vitale, S., Albring, T.A., Pini, M., Gauger, N.R., Colonna, P., et al.: Fully turbulent discrete adjoint solver for non-ideal compressible flow applications. J. Global Power Propul. Soc. **1**, Z1FVOI (2017)
17. Vitale, S., Gori, G., Pini, M., Guardone, A., Economon, T.D., Palacios, F., Alonso, J.J., Colonna, P.: Extension of the SU2 open source CFD code to the simulation of turbulent flows of fuids modelled with complex thermophysical laws. AIAA Paper **2760**, 2015 (2015)